Neural and mammary gland defects in ErbB4 knockout mice genetically rescued from embryonic lethality

Hester Tidcombe*†, Amy Jackson-Fisher†‡, Kathleen Mathers§, David F. Stern‡, Martin Gassmann¶‖, and Jon P. Golding*

*Divisions of Neurobiology and §Biological Services, National Institute for Medical Research, The Ridgeway, Mill Hill, London NW7 1AA, United Kingdom; ‡Department of Pathology, Yale University School of Medicine, New Haven, CT 06520-8023; and ¶Department of Physiology, Biozentrum/Pharmazentrum, University of Basel, Klingelbergstrasse 50, CH-4056 Basel, Switzerland

Edited by Eric N. Olson, University of Texas Southwestern Medical Center, Dallas, TX, and approved May 14, 2003 (received for review October 22, 2002)

Mice lacking the epidermal growth factor receptor family member ErbB4 exhibit defects in cranial neural crest cell migration but die by embryonic day 11 because of defective heart development. To examine later phenotypes, we rescued the heart defects in ErbB4 mutant mice by expressing ErbB4 under a cardiac-specific myosin promoter. Rescued ErbB4 mutant mice reach adulthood and are fertile. However, during pregnancy, mammary lobuloalveoli fail to differentiate correctly and lactation is defective. Rescued mice also display aberrant cranial nerve architecture and increased numbers of large interneurons within the cerebellum.

The epidermal growth factor receptor family member ErbB4 (1) is expressed in many developing and mature organs including heart, breast, and brain (1, 2) and is deregulated in several tumors (3). *In vitro* and dominant negative transgenic studies indicate that ErbB4 stimulates cell survival, proliferation, and differentiation (2, 4–7); in addition recent knockout data demonstrate a role in providing patterning information that is essential for the proper migration of neural crest cells (NCC) and cranial nerve segregation in the developing hindbrain (8–10). The importance of the four ErbB receptors and their various ligands during development has been demonstrated by analysis of loss-of-function mutations in the respective genes: epidermal growth factor receptor (*ErbB1*) (11), *ErbB2* (12–14), *ErbB3* (15, 16), and the ligand neuregulin (nrg-1) (17, 18). Tantalizingly, however, targeted inactivation of ErbB4 results in midembryonic lethality because of failed development of myocardial trabeculae (8). To examine later phenotypes, we rescued the heart defects in ErbB4 mutant mice by expressing human ErbB4 (HER4) under a cardiac-specific myosin promoter. Rescued ErbB4 mutant mice reach adulthood and are fertile. However, during pregnancy, mammary lobuloalveoli fail to differentiate correctly. Stat5, a required component of lobuloalveolar differentiation (19), is not phosphorylated, and lactation is defective. Furthermore, rescued mice display aberrant cranial nerve connections between the facial and trigeminal ganglia and increased numbers of large interneurons within the cerebellum.

Methods

Transgenic Mice. The plasmid cH4M2, containing full-length HER4 cDNA (GenBank L07868, gift of Greg Plowman, Bristol-Myers Squibb), had the HER4 sequence excised by using *Sma*I and *Sna*BI. A polyadenylation (pA) signal was added to the HER4 cDNA by cloning into the *Hin*dIII site of plasmid pβactin, which contains the murine β-actin promoter with an SV40 pA signal (gift of Robb Krumlauf, Stowers Institute for Medical Research, Kansas City, MO). HER4pA was excised using *Sal*I and cloned into the unique *Sal*I site of a plasmid containing the mouse α-myosin heavy chain (αMHC) promoter (gift of James Gulick, University of Cincinnati College of Medicine, Cincinnati; ref. 20). αMHCHER4pA (HER4^{heart}, Fig. 1*A*) was excised by using *Bss*tII and *Not*I and microinjected into fertilized mouse ova, which were placed into the oviducts of pseudopregnant females. DNA from offspring tail samples was genotyped for HER4^{heart} by using PCR primers 5′-AGCTGTGGTCCACATTCTTCAGGA corresponding to nucleotides 728–751 of the second αMHC 5′-untranslated exon (20) and 5′-ACTTGCGCAAGGCTCGGTACTGCT, the reverse complement corresponding to nucleotides 2350–2374 of cH4M2 in the 5′ UTR of HER4 (Fig. 1*B*). A number of lines were found to express the transgene and rescue the embryonic lethality of ErbB4 mutants (8). In this study, one line (HT2) was used for detailed analysis.

RT-PCR. RNA was isolated from embryonic day 10 (E10), E16, P0, and adult tissues by using TRIzol reagent (Invitrogen). Tissues were powdered by pestle and mortar under liquid nitrogen. RNA was DNase-treated, and reverse transcription was performed by using the ThermoScript RT-PCR System (Life Technologies, Grand Island, NY). PCR was performed by using the same primers as HER4^{heart} genotyping, yielding a 500-bp product corresponding to genomic DNA and 250 bp corresponding to cDNA produced by reverse transcriptase. Control PCR used β-actin primer set for RT-PCR, producing a 500-bp cDNA product (Stratagene).

***In Situ* Hybridization.** Whole-mount *in situ* hybridization (21) was performed by using 1 μg/ml digoxigenin-labeled riboprobe at 70°C and visualized with BM-purple substrate (Roche Molecular Biochemicals). *Sox-10* cDNA was a gift of Michael Wegner (Institut für Biochemie, Erlangen, Germany).

Cranial Neurofilament Staining. E11 embryos were processed for whole-mount immunohistochemistry (22) by using 2H3 antineurofilament primary antibody (1:40, Developmental Studies Hybridoma Bank, Iowa City), peroxidase-conjugated goat anti-mouse IgG secondary antibody (1:500, Amersham Pharmacia), and diaminobenzidine chromogen detection. E11 sagittal cryosections were processed with 2H3 antibody, followed by fluorescently labeled secondary antibody (Alexa Fluor 546; 1:300, Molecular Probes).

Whole-Mount Staining of Mammary Glands. Female mice were killed at 5–6 weeks postpartum or 9–10 weeks postpartum. The entire right number 4 inguinal mammary gland was removed and spread onto a glass slide. The mammary gland was fixed in acidic ethanol and stained in Carmine solution as described (23). The stained gland was mounted with Permount (Fisher) and coverslip.

Mammary Gland Histology and Immunohistochemistry. Mammary glands from first or third pregnancy mothers, 1 day postpartum,

This paper was submitted directly (Track II) to the PNAS office.

Abbreviations: αMHC, α-myosin heavy chain; NCC, neural crest cells; NMJ, neuromuscular junction; E*n*, embryonic day *n*.

†H.T. and A.J.-F. contributed equally to this study.

‖To whom correspondence should be addressed. E-mail: Martin.Gassmann@unibas.ch.

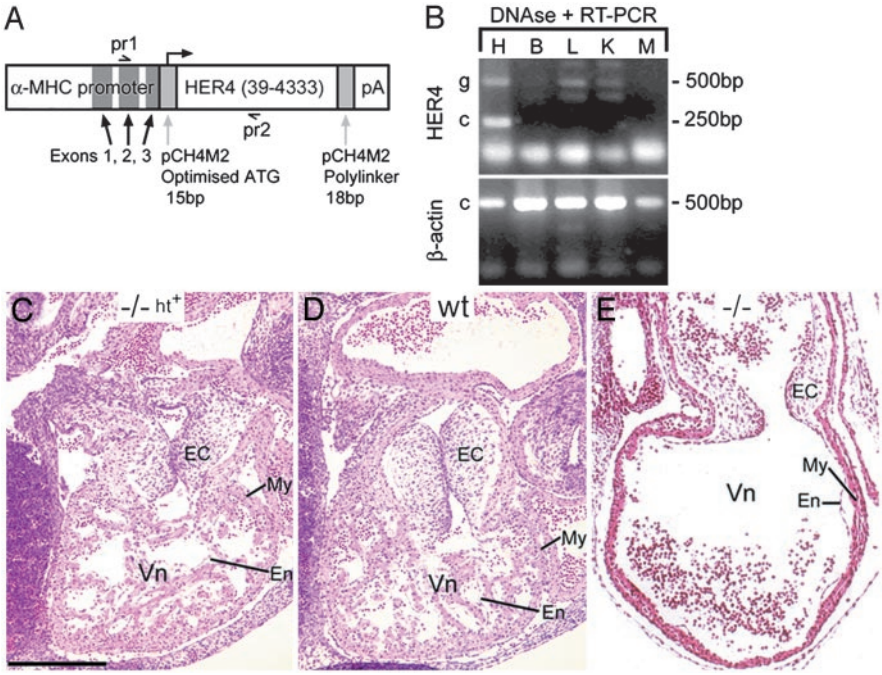

Fig. 1. Production of heart rescue ErbB4$^{-/-}$ mice. (*A*) A DNA construct was made, consisting of human ErbB4 (HER4) cDNA under the control of the α-MHC promoter, and this was injected into mouse ova and transferred to pseudopregnant females. (*B*) Synthesis of transgenic HER4 mRNA within the adult heart (H), but not brain (B), liver (L), kidney (K), or mammary glands (M), was confirmed by RT-PCR amplifying a band of 250 bp. Despite DNase treatment, in some samples a fragment of 500 bp was amplified, indicating contaminating genomic DNA. However, because of the presence of introns in the transgene, amplification products for cDNA (c) and genomic DNA (g) could be clearly separated. The diagnosis of β-actin mRNA was used as a positive control. The HER4^{heart} mouse line was crossed with an ErbB4$^{+/-}$ line to generate ErbB4$^{-/-}$ HER4^{heart} ($-/-$ ht^{+}) offspring in the F_2 generation. (*C* and *D*) Histological examination revealed no differences between E10.5 $-/-$ ht^{+} heart (*C*) and E10.5 WT heart (*D*). This finding contrasts with the dramatic lack of trabeculation within the myocardium (My) of E10.5 ErbB4$^{-/-}$ mice (*E*). My, myocardium; En, endocardium; Vn, ventricle; EC, endocardial cushion. (Scale bar = 0.3 mm.)

were dissected out and fixed overnight in Bouin's solution (for histochemistry) or 4% paraformaldehyde (for immunohistochemistry). Six-micrometer paraffin sections were stained either with hemotoxylin and eosin or processed immunohistochemically as described (7). Primary antibodies were rabbit anti-Stat5a (1:100, AB3163, Chemicon) or goat anti-phosphorylated Stat5 (Tyr-694, 1:100; sc-11761, Santa Cruz Biotechnology). Biotinylated secondary antibodies (Amersham Pharmacia) were used at 1:100 dilutions, and the immunohistochemical signal was enhanced by using Vectastain elite ABC reagent (Vector Laboratories) and developed with diaminobenzidine chromogen before counterstaining with hemotoxylin and eosin.

RNA Isolation and Northern Blot Analysis. Total RNA was isolated from mammary gland tissue snap-frozen in liquid nitrogen and stored at −80°C. Trizol reagent was added to a ratio of 1 ml of Trizol per 0.05 g of frozen tissue. The tissue was homogenized by using a Polytron, and RNA was isolated per the manufacturer's instructions.

To determine expression levels of β-casein, whey acidic protein, and α-lactalbumin, 10 μg of total RNA was separated on a 1.0% denaturing agarose gel and transferred to BrightStar-Plus nylon membrane (Ambion) with the NorthernMax kit (Ambion). RNA was crosslinked to the membrane with a Stratagene UV Stratalinker. DNA probes for β-casein, whey acidic protein, and α-lactalbumin (plasmids provided by Frank Jones, Tulane University, New Orleans) and GAPDH (Invitrogen) were labeled with [α-^{32}P]dCTP (Redivue, Amersham Pharmacia) by using the Random-Primed DNA labeling kit and mini Quick Spin DNA columns (both from Roche Molecular Biochemicals) per the manufacturer's instructions. The probes were hybridized to the membrane overnight and washed as instructed by NorthernMax kit (Ambion). The membrane was exposed to a PhosphoImager screen, and quantitation of specific RNA expression was determined with IMAGEQUANT software. The membranes were stripped and rehybridized with GAPDH cDNA for loading normalization.

Cerebellum Immunohistochemistry. Sagittal sections of adult cerebellum were stained with either 2H3 antineurofilament antibody (1:40) or rabbit antisomatostatin antibody (1:100, AB5494, Chemicon), followed by biotinylated secondary antibody and ABC/diaminobenzidine detection, as described above, and thionin counterstain.

Results and Discussion

Generation of HER4^{heart} Transgenic Mice. Transgenic mice expressing human ErbB4 (HER4) cDNA under the control of the cardiac-specific α-MHC promoter (Fig. 1*A*) were created by pronuclear injection. Several lines were established, which transmitted the transgene in a Mendelian fashion and exhibited no overt phenotype. Expression of the transgene was assessed in one line by RT-PCR (Fig. 1*B*). This finding demonstrates that HER4^{heart} transgene mRNA is expressed in adult heart, but not brain, liver, kidney, or mammary gland. At earlier stages of development (E10, E16, P0), HER4^{heart} expression is similarly absent from noncardiac tissues (data not shown). Thus, at all ages examined, transgene expression was exclusively observed in the heart.

Cardiac Defects Are Rescued in ErbB4$^{-/-}$ HER4^{heart} Mice. HER4^{heart} transgenic mice crossed with ErbB4$^{+/-}$ mice yielded viable ErbB4$^{-/-}$ HER4^{heart} mice among the offspring of the F_2 generation, showing that the heart defect had been circumvented.

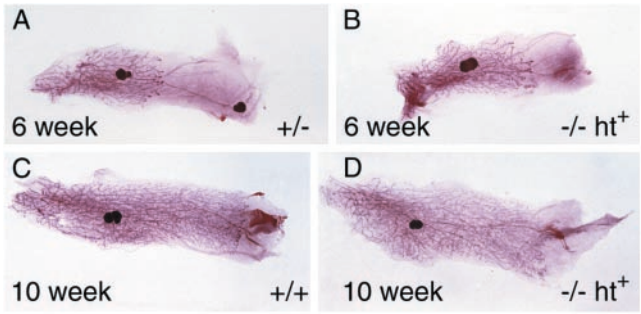

Fig. 2. Whole-mount analysis of no. 4 inguinal mammary glands from pubescent females. Glands were extracted from 5- to 6-week-old (*A* and *B*, $n = 26$) and 9- to 10-week-old (*C* and *D*, $n = 21$) littermates and stained with Carmine Alum. Ductal branching and elongation were similar among all genotypes.

However, fewer rescued ErbB4 mutant pups were born than predicted by Mendelian genetics (39 $-/-$ born of 261 total; predicted: 61 $-/-$, χ^2 test, $P = 0.0001$).

Transverse sections of E10.5 ErbB4$^{-/-}$ HER4^{heart} heart (Fig. 1*C*) show trabeculation indistinguishable from WT (Fig. 1*D*), unlike the dramatic lack of trabeculation in E10.5 ErbB4$^{-/-}$ heart (Fig. 1*E*). It is possible that in some ErbB4$^{-/-}$ HER4^{heart} embryos, transgene expression is not sufficient to completely restore all functions of trabeculation required during growth (24), explaining the reduced numbers of ErbB4 mutant pups observed. Transgenic expression of HER4 in the myocardial muscle results in normal morphology of adult ErbB4$^{-/-}$ HER4^{heart} hearts, including atrioventricular valves (data not shown). Similarly, Morris and colleagues (13) could prevent the formation of trabeculation defects in ErbB2 knockout mice by reintroducing ErbB2 into the myocardium using the same 5.5-kb αMHC promoter element. Thus, it is very likely that ErbB2/4 heterodimers in the myocardium are crucial for the transduction of neuregulin signals from the endocardium during trabeculation in the embryonic heart (25). This finding is in contrast to the function of ErbB3, which is expressed in the mesenchyme of the endocardial cushion. Defects in atrioventricular valve formation were reported in one of the two ErbB3 knockout lines generated, resulting in embryonic lethality at E13.5 (16). However, in the other line, similar defects were not observed, and a large proportion of ErbB3$^{-/-}$ mice developed to term (15).

Aberrant Mammary Gland Maturation and Requirement of ErbB4 for Stat5 Phosphorylation. Offspring of ErbB4$^{-/-}$ HER4^{heart} mothers showed a marked perinatal lethality, with 82% of pups (36 of 44) becoming emaciated and dying between birth and P10, compared with an average 3% (5 of 172) death rate in pups born to ErbB4$^{+/-}$ HER4^{heart} mothers. Dying pups were of all genotypes and survived when fostered with ErbB4$^{+/-}$ mothers, indicating that the problem lay with the ErbB4$^{-/-}$ HER4^{heart} mothers. Such maternal phenotypes could be behavioral or reflect a defect in mammopoiesis and/or lactation.

To address whether establishment of the ductal tree during puberty is affected, we performed whole-mount staining of right inguinal (no. 4) mammary glands at multiple stages. In sibling comparisons at 5–6 weeks postnatal, mammary gland development of ErbB4$^{-/-}$ HER4^{heart} mice often outpaced that of ErbB4$^{+/-}$ and WT siblings, but there was considerable variability. However, at 9–10 weeks postnatal, development of the ductal tree was similar among all genotypes (Fig. 2). (Although terminal end buds are visible in the glands pictured, in all other cases the terminal end buds had regressed by this time point.) Subsequently, we investigated whether proliferation and/or differentiation of the mammary epithelium during pregnancy was

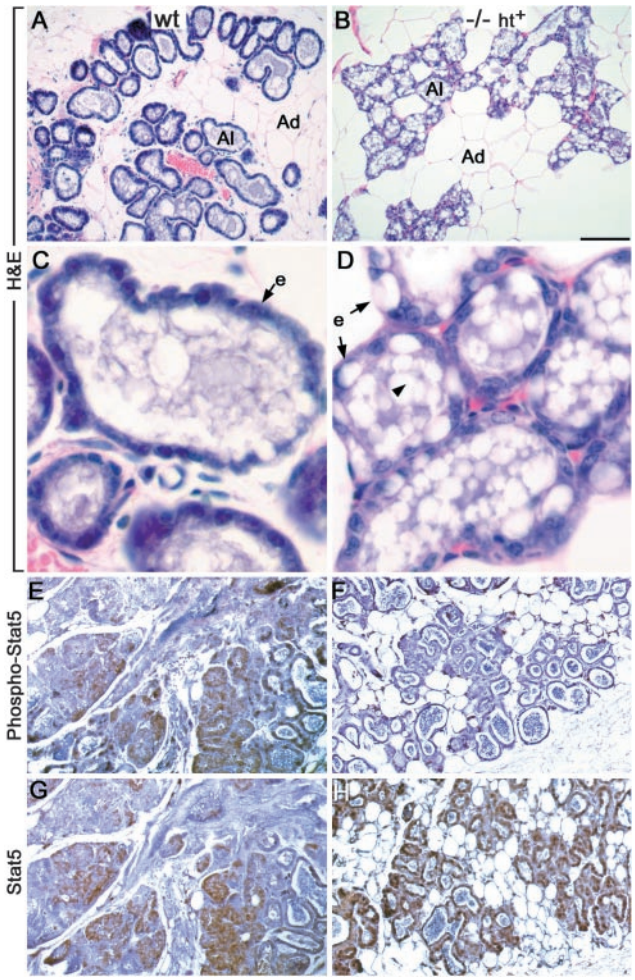

Fig. 3. Aberrant mammary gland histology and lack of phosphorylated Stat5 in postpartum ErbB4$^{-/-}$ HER4^{heart} females. Histochemical and immunohistochemical analysis was performed on sections of WT (*A*, *C*, *E*, and *G*) or ErbB4$^{-/-}$ HER4^{heart} ($-/-$ ht^{+}) (*B*, *D*, *F*, and *H*) inguinal (no. 4) mammary glands. (*A–D*) Low-power (*A* and *B*) and higher-power (*C* and *D*) views of hematoxylin and eosin stained 1 day postpartum, third pregnancy mammary gland. Note the poorly differentiated alveolar epithelial cells (e, arrows) and lipid-filled alveoli (Al) in $-/-$ ht^{+} mammary glands. (*E–H*) Anti-phospho-Stat5 antibody revealed a lack of Stat5 phosphorylation in 1 day postpartum, first pregnancy mammary glands from $-/-$ ht^{+} females (*F*), which is detectable in WT (*E*). However, anti-Stat5a antibody revealed that Stat5 was present in both WT (*G*) and mutant (*H*) alveolar epithelia. Ad, adipocyte. (Scale bar = 0.1 mm.)

affected in mutant glands. Histology of the inguinal (no. 4) mammary glands of third-litter ErbB4$^{-/-}$ HER4^{heart} mothers 1 day postpartum revealed abnormal alveolar organization (Al, Fig. 3 *A–D*). Alveolar epithelial cells (e, arrows in Fig. 3 *C* and *D*) do not form a coherent boundary and are not columnar. Lipid globules fill up most of the lumens (arrowhead in Fig. 3*D*), and are also trapped inside epithelial cells (arrows in Fig. 3*D*), implying that epithelial cell differentiation, which normally occurs in late pregnancy, has been disrupted. Such an observation is consistent with defective lactation. Thus, we analyzed the expression of major milk genes by Northern blot analysis. Expression of whey acidic protein (WAP), α-lactalbumin, and β-casein was moderately (20–30%) lower in ErbB4$^{-/-}$ HER4^{heart} glands than in ErbB4$^{+/-}$ and WT glands at day 1 lactation when normalized to GAPDH loading controls (data not shown). This finding suggests that the impaired lactation is not necessarily a consequence of reduced milk gene production but may rather reflect a failure in secretory maturation of the alveoli.

Targeted inactivation of the *Stat5a* gene demonstrated that this transcription factor is a major player controlling mammary gland development and differentiation (19). Furthermore, Stat5 tyrosine phosphorylation occurs in tissue culture when Stat5 is jointly expressed with ErbB4 (7). Therefore, we examined Stat5 phosphorylation immunohistochemically in inguinal (no. 4) mammary gland sections of first-litter mothers 1 day postpartum. Stat5 phosphorylation was absent in ErbB4$^{-/-}$ HER4^{heart} mammary glands (Fig. 3*F*), although Stat5a protein was distributed normally (Fig. 3*H*), in contrast to WT, where Stat5 is phosphorylated (Fig. 3 *E* and *G*).

Our results contribute to mounting evidence that the phosphorylation of Stat5, which is an essential requirement for alveolar differentiation and lactation in the mammary gland (26), is not exclusively controlled by prolactin receptor activation (4). Stat5 phosphorylation has been reported in response to other stimuli, such as growth hormone and epidermal growth factor (27) and the ErbB ligands neuregulin and amphiregulin (7). Accordingly, down-regulation of ErbB receptor signaling using a dominant negative approach in mice prevented Stat5 phosphorylation; however, specific phenotypes did not develop until midlactation (7). Furthermore, mammary gland-specific ErbB4 knockout mice have been created (W. Long, K. U. Wagner, K. C. K. Lloyd, N. Binart, L. Hennighausen, and F. E. Jones, personal communication), which show the same lack of Stat5 phosphorylation as our mice and similar failure of lactation. ErbB receptors have also been shown to activate Stat5 *in vitro* (7, 28). Therefore, we conclude that ErbB4 is required for alveolar differentiation and maintenance in late pregnancy and lactation and that it is a dominant regulator of Stat5 activation.

Aberrant Cranial Neural Crest Migration and Cranial Nerve Architecture. Within the developing hindbrain, cranial NCC emigrate from rhombomeres (r)2, r4, and r6 into the adjacent cranial mesenchyme in three segregated streams (29). ErbB4 is expressed within r3 and r5, but in embryos lacking ErbB4, aberrant migration of some r4 NCC and aberrant axon pathfinding into r3-adjacent mesenchyme is seen between E8.5 and E10.5 (8, 10). Comparison of ErbB4$^{+/-}$ HER4^{heart} and ErbB4$^{-/-}$ HER4^{heart} embryos using *Sox10 in situ* hybridization as a diagnostic marker for NCC (30, 31) demonstrated a similar aberrant migration of a subpopulation of r4 NCC into r3-adjacent cranial mesenchyme in ErbB4$^{-/-}$ HER4^{heart} embryos. Aberrantly migrating *Sox10*-expressing cells are observed beginning E8.5 (compare Fig. 4 *A* and *B*, arrow in *B*) and connect the r4 and r2 NCC streams by E9 (compare Fig. 4 *C* and *D*, arrow in *D*). By E11, 2H3 neurofilament antibody staining demonstrated aberrantly projecting axons extending through r3-adjacent mesenchyme, connecting the geniculate/cochleovestibular (gVII/gVIII) ganglion complex with the trigeminal (gV) ganglion (compare whole mounts in Fig. 4 *E* (+/− ht$^+$) and *F* (−/− ht$^+$) and mutant sagittal section 3G), replicating the phenotype of E10.5 ErbB4$^{-/-}$ embryos (8). Histological analysis at E17.5 revealed that ectopic nerve projections persist and result in an ectopic cranial nerve between the geniculate (gVII) and trigeminal (gV) ganglia (Fig. 5, arrow in *C*). However, the position of the ganglia themselves is normal, and no other anatomical changes could be identified. By injecting DiI into caudal gV at E17.5 and allowing 1 month for dye diffusion, labeled axons were seen within gVII and the facial nerve (compare Fig. 5 *E* and *F*, arrow in *E*). Hence, aberrantly projecting neurons survive the phase of refinement when the axons reach the vicinity of their targets during late embryogenesis, which is marked by naturally occurring neuronal death (32). Interestingly, similar aberrant cranial nerve connections occasionally occur in humans: V-III nerve connection (Marcus–Gunn syndrome) (33) and V-VII nerve connection (34). NCC also contribute to the cartilaginous structures of the head. However, newborn ErbB4$^{-/-}$ HER4^{heart} skulls demonstrated no obvious abnormalities of the cranial skeleton or inner ear (data not shown). A recent study using our ErbB4$^{-/-}$ HER4^{heart} mice similarly found no abnormalities in lower jaw or tooth development (35).

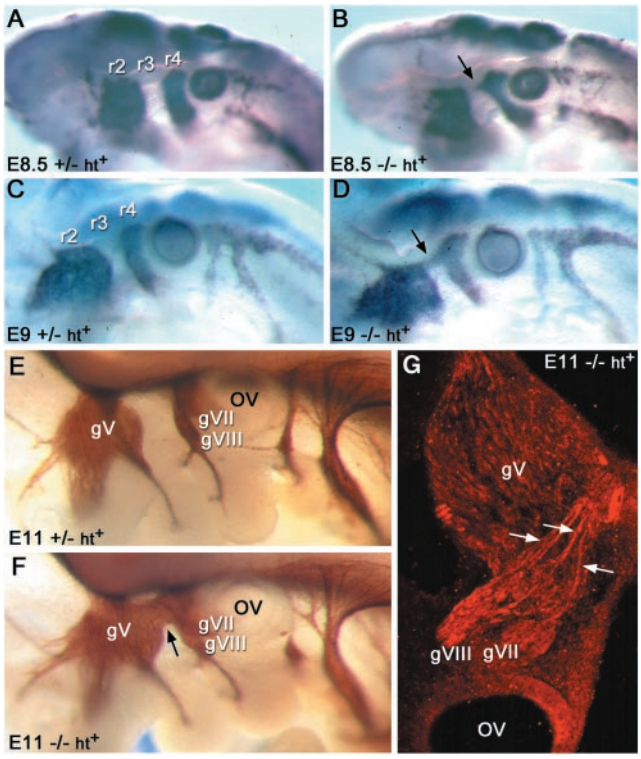

Fig. 4. Aberrant cranial NCC migration and axon pathfinding. Whole-mount *in situ* hybridization with the NCC marker *Sox10* on E8.5 (*A* and *B*) and E9 (*C* and *D*) embryos revealed aberrant migration of r4-derived NCCs (arrow in *B* and *D*) rostrally into mesenchyme adjacent to r3 only in ErbB4$^{-/-}$ HER4^{heart} embryos. (*E* and *F*) By E11, whole-mount 2H3 antineurofilament immunohistochemistry revealed an ectopic cranial nerve (arrow in *F*) connecting the geniculate/cochleovestibular (gVII/gVIII) and trigeminal (gV) ganglia in ErbB4$^{-/-}$ HER4^{heart} embryos (*F*). (*G*) Ectopic nerve fibers are clearly visible (arrows) in a sagittal section through the hindbrain, stained with 2H3 antibody, and detected with a fluorescent secondary antibody. OV, otic vesicle.

Cerebellum Defects. The granular layer of the cerebellar cortex consists of densely packed neuronal cells. They are classified into two major morphologically and functionally distinct neuronal types: small granule cells and large interneurons. Analysis of adult cerebellum revealed no differences in the distribution of granule cells between ErbB4$^{-/-}$ HER4^{heart} and ErbB4$^{+/-}$ HER4^{heart} cerebellum (Fig. 6), conflicting with the *in vitro* requirement of neuregulin/ErbB4 for granule cell migration (6). However, we observed significantly increased numbers of large interneurons in the granule cell layer of ErbB4$^{-/-}$ HER4^{heart} animals (arrows in Fig. 6). Thus, using anatomically matched 6-μm sections (122 sections per genotype from three animals per genotype), we found 4,483 large interneurons in ErbB4$^{-/-}$ HER4^{heart} adults compared with 3,114 in ErbB4$^{+/-}$ HER4^{heart} adults (t test, $P = 0.0003$). Sizes of these large interneurons were not significantly different (data not shown), ruling out hypertrophy as an explanation for the increased number of cell profiles per section. In an attempt to further characterize this phenotype, we performed antisomatostatin immunohistochemistry identifying Golgi cells as a likely neuronal population affected (arrows in Fig. 6 *C* and *D*) (36). ErbB4 is expressed within the granule cell layer, but it remains unconfirmed in large interneurons (37). If large interneurons expressed ErbB4, then the phenotype could

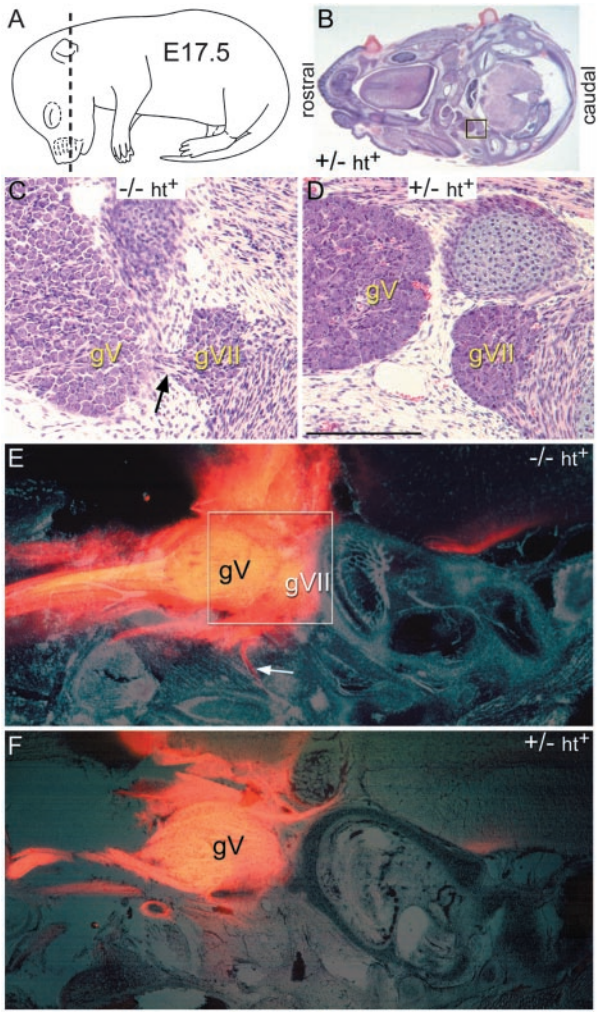

Fig. 5. Persistence of aberrant cranial nerve connections. Horizontal sections through the head of E17.5 embryos (plane of section shown in *A*) were stained with hematoxylin and eosin. (*B*) Low-power view of a ErbB4$^{+/-}$ HER4^{heart} head section with a box showing the region magnified in *C* and *D*. Comparisons of ErbB4$^{-/-}$ HER4^{heart} (*C*) and ErbB4$^{+/-}$ HER4^{heart} (*D*) embryos reveal an aberrant connection persisting between the geniculate (gVII) and trigeminal (gV) ganglia in heart rescue mutants (arrow in *C*). (*E* and *F*) DiI was focally injected into caudal gV and revealed aberrant nerve connections between gV and gVII and also labeled the facial nerve in $-/-$ ht$^+$ embryos (arrow in *E*) but not in $+/-$ ht$^+$ embryos (*F*). (Scale bar = 0.25 mm.)

be cell autonomous, with ErbB4 regulating cell differentiation, and in its absence the proliferative phase of cell development might therefore be prolonged.

Neuromuscular Junctions (NMJ) Develop Normally. ErbB2, ErbB3, and ErbB4 all are expressed in muscle cells and concentrated at NMJ (38–41). They are thought to be involved in the expression and clustering of acetylcholine receptors in conjunction with agrin and the receptor tyrosine kinase MuSK (42). Within the diaphragm of ErbB2 heart rescue or ErbB3$^{-/-}$ mice, NMJ are disorganized, and the phrenic nerve is absent (13, 14, 16). However, this phenotype caused by a defect in Schwann cell development and subsequent motor neuron degeneration. Thus, it was observed that postsynaptic development of the NMJ is

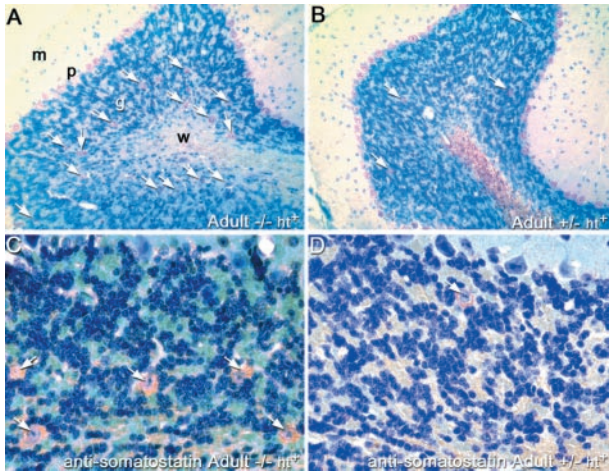

Fig. 6. Abnormal cerebellum anatomy. Adult ErbB4$^{-/-}$ HER4^{heart} (*A* and *C*) and adult ErbB4$^{+/-}$ HER4^{heart} (*B* and *D*) cerebellum lightly stained with 2H3 antineurofilament antibody (*A* and *B*) or antisomatostatin antibody (*C* and *D*) and counterstained with thionin. Many more large-diameter somatostatin immunoreactive cells are seen within the $-/-$ ht$^+$ granule cell layer than within the $+/-$ ht$^+$ granule cell layer (arrows). Various layers are labeled in *A*: m (molecular layer), p (Purkinje cells), g (granule cells), and w (white matter).

largely unaffected in these mice. We found no differences in phrenic nerve or NMJ organization between diaphragms of newborn ErbB4$^{-/-}$ HER4^{heart} and ErbB4$^{+/-}$ HER4^{heart} animals (data not shown), indicating that ErbB4 is not essential for pre- and postsynaptic development of the NMJ. In light of the changing view of neuromuscular synapse formation, the role of the neuregulin/ErbB signaling module in this process is presently unclear.

Conclusion

Rescue of the cardiac defects in ErbB4 mutant mice provides a valuable tool to study the function of ErbB4 during developmental processes and in the homeostasis of mature organs. In particular, our analysis reveals important roles for ErbB4 in morphogenesis of the mammary gland and nervous system development and improves our understanding of the interactions between ErbB4 and other ErbB family members. ErbB involvement in heart trabeculation is very likely limited to the ErbB2/ErbB4 heterodimer, whereas ErbB2/ErbB3 is the neuregulin receptor required for Schwann cell development. The importance of this neuregulin receptor in development of the peripheral nervous system is illustrated by the observation that down-regulation of ErbB3 accounts for many of the neural crest defects in *Sox10* mutant mice (31). Finally, because the specific hindbrain defects in ErbB4$^{-/-}$ HER4^{heart} rescue mice are not seen in other ErbB receptor or neuregulin loss-of-function animals, our data provide strong *in vivo* evidence for signal transduction events mediated by ErbB4 homodimers.

We thank Frank Jones for communicating unpublished results and critically reviewing the manuscript, Josef Kapfhammer for expert advice on cerebellum anatomy, Monica Dixon and Vicky Tsoni for helpful discussions, Gary Bellinger for expert technical assistance, and Ian Harragan and Elena Grigorieva for excellent histology. This work was funded by core program support from the Medical Research Council (U.K.), U.S. Army Medical Research Acquisition Activity (U.S. Department of the Army, Fort Detrick, MD) Grant DAMD 17-99-1-9459 (to A.J.-F.); and U.S. Public Health Service Grant RO1CA80065 from the National Cancer Institute (to D.F.S.).

1. Plowman, G. D., Culouscou, J. M., Whitney, G. S., Green, J. M., Carlton, G. W., Foy, L., Neubauer, M. G. & Shoyab, M. (1993) *Proc. Natl. Acad. Sci. USA* **90,** 1746–1750.
2. Yarden, Y. & Sliwkowski, M. X. (2001) *Nat. Rev. Mol. Cell Biol.* **2,** 127–137.
3. Mason, S. & Gullick, W. J. (1995) *Breast* **4,** 11–18.
4. Troyer, K. L. & Lee, D. C. (2001) *J. Mammary Gland Biol. Neoplasia* **6,** 7–21.

5. Burden, S. & Yarden, Y. (1997) *Neuron* **18,** 847–855.
6. Rio, C., Rieff, H. I., Qi, P. & Corfas, G. (1997) *Neuron* **19,** 39–50.
7. Jones, F. E., Welte, T., Fu, X. Y. & Stern, D. F. (1999) *J. Cell Biol.* **147,** 77–88.
8. Gassmann, M., Casagranda, F., Orioli, D., Simon, H., Lai, C., Klein, R. & Lemke, G. (1995) *Nature* **378,** 390–394.
9. Golding, J. P., Tidcombe, H., Tsoni, S. & Gassmann, M. (1999) *Dev. Biol.* **216,** 85–97.
10. Golding, J. P., Trainor, P., Krumlauf, R. & Gassmann, M. (2000) *Nat. Cell. Biol.* **2,** 103–109.
11. Sibilia, M. & Wagner, E. F. (1995) *Science* **269,** 234–238.
12. Lee, K. F., Simon, H., Chen, H., Bates, B., Hung, M. C. & Hauser, C. (1995) *Nature* **378,** 394–398.
13. Morris, J. K., Lin, W., Hauser, C., Marchuk, Y., Getman, D. & Lee, K. F. (1999) *Neuron* **23,** 273–283.
14. Woldeyesus, M. T., Britsch, S., Riethmacher, D., Xu, L., Sonnenberg-Riethmacher, E., Abou-Rebyeh, F., Harvey, R., Caroni, P. & Birchmeier, C. (1999) *Genes Dev.* **13,** 2538–2548.
15. Riethmacher, D., Sonnenberg-Riethmacher, E., Brinkmann, V., Yamaai, T., Lewin, G. R. & Birchmeier, C. (1997) *Nature* **389,** 725–730.
16. Erickson, S. L., O'Shea, K. S., Ghaboosi, N., Loverro, L., Frantz, G., Bauer, M., Lu, L. H. & Moore, M. W. (1997) *Development (Cambridge, U.K.)* **124,** 4999–5011.
17. Meyer, D. & Birchmeier, C. (1995) *Nature* **378,** 386–390.
18. Kramer, R., Bucay, N., Kane, D. J., Martin, L. E., Tarpley, J. E. & Theill, L. E. (1996) *Proc. Natl. Acad. Sci. USA* **93,** 4833–4838.
19. Liu, X., Robinson, G., Wagner, K., Garrett, L., Wynshaw-Boris, A. & Henninghausen, L. (1997) *Genes Dev.* **11,** 179–186.
20. Gulick, J., Subramaniam, A., Neumann, J. & Robbins, J. (1991) *J. Biol. Chem.* **266,** 9180–9185.
21. Grove, E. A., Tole, S., Limon, J., Yip, L.-W. & Ragsdale, C. W. (1998) *Development (Cambridge, U.K.)* **125,** 2315–2325.
22. Lumsden, A. & Keynes, R. (1989) *Nature* **337,** 424–428.
23. Jones, F. E., Jerry, D. J., Guarino, B. C., Andrews, G. C. & Stern, D. F. (1996) *Cell Growth Differ.* **7,** 1031–1038.
24. Sedmera, D. & Thomas, P. S. (1996) *BioEssays* **18,** 607.
25. Sedmera, D., Pexieder, T., Vuillemin, M., Thompson, R. P. & Anderson, R. H. (2000) *Anat. Rec.* **258,** 319–337.
26. Miyoshi, K., Shillingford, J. M., Smith, G. H., Grimm, S. L., Wagner, K. U., Oka, T., Rosen, J. M., Robinson, G. W. & Henninghausen, L. (2001) *J. Cell Biol.* **155,** 531–542.
27. Gallego, M. I., Binart, N., Robinson, G. W., Okagaki, R., Coschigano, K. T., Perry, J., Kopchick, J. J., Oka, T., Kelly, P. A. & Henninghausen, L. (2001) *Dev. Biol.* **229,** 163–175.
28. Olayioye, M. A., Beuvink, I., Horsch, K., Daly, J. M. & Hynes, N. E. (1999) *J. Biol. Chem.* **274,** 17209–17218.
29. Trainor, P. A. & Krumlauf, R. (2000) *Nat. Rev. Neurosci.* **1,** 116–124.
30. Kuhlbrodt, K., Herbarth, B., Sock, E., Hermans-Borgmeyer, I. & Wegner, M. (1998) *J. Neurosci.* **18,** 237–250.
31. Britsch, S., Goerich, D. E., Riethmacher, D., Peirano, R. I., Rossner, M., Nave, K. A., Birchmeier, C. & Wegner, M. (2001) *Genes Dev.* **15,** 66–78.
32. Buchman, V. L. & Davies, A. M. (1993) *Development (Cambridge, U.K.)* **118,** 989–1001.
33. Pratt, S. G., Beyer, C. K. & Johnson, C. C. (1984) *Ophthalmology* **91,** 27–30.
34. Cheney, M. L., McKenna, M. J., Megerian, C. A., West, C. & Elahi, M. M. (1997) *Ann. Otol. Rhinol. Laryngol.* **106,** 733–738.
35. Fried, K., Risling, M., Tidcombe, H., Gassmann, M. & Lillesaar, C. (2002) *Dev. Dyn.* **224,** 356–360.
36. Geurts, F. J., Timmermans, J., Shigemoto, R. & De Schutter, E. (2001) *Neuroscience* **104,** 499–512.
37. Ozaki, M., Kishigami, S. & Yano, R. (1998) *Neurosci. Res.* **30,** 351–354.
38. Altiok, N., Bessereau, J. L. & Changeux, J. P. (1995) *EMBO J.* **14,** 4258–4266.
39. Jo, S. A., Zhu, X., Marchionni, M. A. & Burden, S. J. (1995) *Nature* **373,** 158–161.
40. Moscoso, L. M., Chu, G. C., Gautam, M., Noakes, P. G., Merlie, J. P. & Sanes, J. R. (1995) *Dev. Biol.* **172,** 158–169.
41. Zhu, X., Lai, C., Thomas, S. & Burden, S. J. (1995) *EMBO J.* **14,** 5842–5848.
42. Burden, S. J. (1998) *Genes Dev.* **12,** 133–148.